

Article

Overcoming the Trade-Off between Methanol Rejection and Proton Conductivity via Facile Synthesis of Crosslinked Sulfonated PEEK Proton Exchange Membranes

Stef Depuydt ¹, Lucy Traub ², Gilles Van Eygen ¹, Santosh Kumar ³, Georg Held ³ and Bart Van der Bruggen ^{1,*}

¹ Department of Chemical Engineering, KU Leuven, Celestijnenlaan 200F, B-3001 Leuven, Belgium; stef.depuydt@kuleuven.be (S.D.)

² Department of Chemical Engineering, The Pennsylvania State University, University Park, PA 16802, USA

³ Diamond Light Source Ltd., Harwell Science and Innovation Campus, Fermi Ave, Didcot OX11 0DE, UK; georg.held@diamond.ac.uk (G.H.)

* Correspondence: bart.vanderbruggen@kuleuven.be

Abstract: In this work, homogeneous, thin-film proton exchange membranes (PEMs) with superior proton conductivities and high methanol rejection were fabricated via a facile synthesis procedure. Sulfonated polyether ether ketone (sPEEK) was crosslinked via a Friedel–Crafts reaction by α,α' -dichloro-p-xylene, a non-hazardous and hydrophobic compound. PEMs with varying crosslinking and sulfonation degrees were fabricated to overcome the traditional trade-off between methanol rejection and proton conductivity. The sulfonation of PEEK at 60 °C for 24 h resulted in a sulfonation degree of 56%. Those highly sulfonated backbones, in combination with a low membrane thickness (ca. 20 μm), resulted in proton conductivities superior to Nafion 117. Furthermore, X-ray photoelectron spectroscopy proved it was possible to control the crosslinking degree via the crosslinking time and temperature. The PEMs with the highest crosslinking degree showed better methanol rejection compared to the commercial benchmark. The introduction of the crosslinker created hydrophobic membrane sections, which reduced the water and methanol uptake. Subsequently, the membrane became denser due to the crosslinking, hindering the solute permeation. Those two effects led to lower methanol crossovers. This study proved the successful fabrication of PEMs overcoming the trade-off between proton conductivity and methanol rejection, following a facile procedure using low-cost and non-hazardous materials.

Keywords: electrochemistry; membrane synthesis; cation exchange membrane; proton conductivity; polyether ether ketone; methanol retention



Citation: Depuydt, S.; Traub, L.; Van Eygen, G.; Kumar, S.; Held, G.; Van der Bruggen, B. Overcoming the Trade-Off between Methanol Rejection and Proton Conductivity via Facile Synthesis of Crosslinked Sulfonated PEEK Proton Exchange Membranes. *Appl. Sci.* **2024**, *14*, 3089. <https://doi.org/10.3390/app14073089>

Academic Editor: Adrian Irimescu

Received: 26 February 2024

Revised: 30 March 2024

Accepted: 3 April 2024

Published: 7 April 2024



Copyright: © 2024 by the authors. Licensee MDPI, Basel, Switzerland. This article is an open access article distributed under the terms and conditions of the Creative Commons Attribution (CC BY) license (<https://creativecommons.org/licenses/by/4.0/>).

1. Introduction

In the last decades, climate change has become one of the major challenges of the modern world. Rising sea levels, droughts, increases in greenhouse gas emissions, and scarcity of resources confront the current generations with grave and pressing challenges. For those reasons, a new technological revolution towards clean and sustainable transport, energy sources, and industries is taking place [1]. The development of direct methanol fuel cells (DMFCs) and artificial photosynthesis is part of that technological revolution. The purpose of DMFCs is to generate energy using methanol as fuel, and artificial photosynthesis is used to generate fuel from energy with the aid of sunlight. Both technologies make use of an electrochemical cell, commonly equipped with a proton exchange membrane (PEM). Within a DMFC, methanol is oxidized in the anode compartment, which generates electrons and protons. The electrons carrying the free energy travel via an external circuit towards the cathode, which generates a potential difference. To maintain the charge balance, the protons also need to be transported to the cathode compartment through a semi-permeable membrane, i.e., a PEM [2,3]. On the other hand, within artificial photosynthesis, CO₂ is

reduced in the cathode compartment under the influence of an external potential difference and sunlight. Possible reaction products are methanol, ethanol, and ethylene. Similarly to DMFCs, the charge balance is maintained by transporting protons from the anode to the cathode compartment using a PEM [4,5].

PEMs are dense, semi-permeable membranes commonly fabricated from polymers containing fixed, negatively charged groups that give preference to proton transport while rejecting other compounds. Nowadays, perfluorinated PEMs, such as the commercial Nafion membranes, are the most commonly employed PEMs for DMFC and artificial photosynthesis [2,4–6]. They show high proton conductivities due to their phase-separated morphology, i.e., a hydrophobic backbone combined with hydrophilic side chains, and their high ion exchange capacity (IEC) [2,5,7,8]. Furthermore, these membranes have high thermal and chemical stability. However, Nafion has certain limitations, making it unsuitable for a broader application range. The main drawbacks are its high methanol permeability [6,9,10] and high production cost [9–12]. In addition, it contributes to global PFAS pollution, endangering human health and the environment [13–16].

Extensive research has been undertaken on alternative polymers to replace the perfluorinated membranes. Polyether ether ketone (PEEK) is a low-cost polymer, showing good film-forming properties and easy sulfonation [17–23]. Generally, sulfonic acid groups are used as the functional groups in PEMs. The combination of these polar groups and the hydrophobic aromatic backbone provides the membrane with a phase-separated structure [24]. Recently, many efforts have been devoted to preparing the membranes with dense structures to minimize the solvent absorption rates and swelling degrees [25]. Crosslinking the polymer leads to a dense, tortuous 3D network with steric effects, which leads to decreased swelling. Additionally, a crosslinked membrane structure shows increased cation/anion permeation, lowers the hydrogen and methanol crossover, and enhances the thermal and mechanical stability [26,27]. Various studies on employing sulfonated PEEK (sPEEK) as the polymer backbone have already been performed [17–23]. For example, Li et al. [21] synthesized self-crosslinked sPEEK membranes with sulfonic acid groups on the aliphatic side chains. They used concentrated sulfuric acid to perform the sulfonation, after which the sPEEK was reduced with borohydride. The pending sulfoalkoxy groups were added by using 1,3-propane sultone. Their results showed an even higher proton conductivity than Nafion 212. However, despite that good performance, two consecutive solvent steps, in addition to the sulfonation step, were required for the membrane synthesis, complicating the fabrication process. Furthermore, various toxic chemicals, such as borohydride and 1,3-propane sultone, were used during the synthesis. Furthermore, the authors did not report the methanol permeability, which is a crucial parameter for applications such as DMFCs and artificial photosynthesis. Zhong et al. [22] synthesized sPEEK membranes crosslinked via UV light using benzophenone (BP) and triethylamine (TEA) as the photo-initiator. Similarly, due to the use of diallyl bisphenol, they were not able to avoid toxic chemicals as membrane polymer building blocks. Wang et al. [23] used a polymer that only showed a weakly phase-separated structure, leading to inadequate proton conductivity. Zhao et al. [18] sulfonated PEEK using concentrated sulfuric acid and crosslinked the polymer using benzoxazine. The obtained membranes showed good methanol permeability and proton conductivity, but a trade-off was necessary for those two parameters. With an increasing crosslinking degree, the methanol permeability ranged between 5.79×10^{-5} and 5.46×10^{-7} cm²/s, and the proton conductivity ranged between 7.76×10^{-2} and 1.61×10^{-4} S/cm, whilst the commercial Nafion 117 membrane has a methanol permeability and proton conductivity equal to 1.88×10^{-6} cm²/s and 0.0891 S/cm, respectively. Again, the use of toxic compounds, such as aniline, paraformaldehyde, and bisphenol A, was required to synthesize the membranes. In another study by Zhao et al. [19], more inexpensive and safer chemicals were used for the crosslinking, i.e., styrene, divinylbenzene and AIBN. The resulting membranes showed competitive results compared to Nafion, but they were again not able to obtain a membrane that simultaneously showed better methanol retention and proton conductivity compared to the commercial benchmark.

This study aims at tackling the main limitations of the current PEMs, i.e., overcoming the trade-off between methanol rejection and proton conductivity, whilst only using non-hazardous, low-cost chemicals for the PEM synthesis. Methanol crossover and proton conductivity are two key performance parameters of a PEM. More specifically, methanol crossover is seen as one of the most notable technical barriers causing performance losses, whilst the proton conductivity is in direct relation to the energy requirements of a system [28]. This study employed α,α' -dichloro-p-xylene (DCX) as a low-cost, non-hazardous crosslinker. The chloromethyl groups on the benzene ring of DCX enable a Friedel–Crafts reaction between DCX and the aromatic rings of the sPEEK backbone. Additionally, the hydrophobic character of DCX can lower the methanol crossover. To the best of our knowledge, DCX has not been used in the fabrication of PEMs or in the crosslinking of sPEEK. It has only been used in a limited number of studies for the crosslinking of nanofiltration membranes [29,30]. Furthermore, thin film PEMs having a highly sulfonated PEEK backbone will be fabricated in order to limit the proton resistance.

2. Materials and Methods

2.1. Materials

Polyether ether ketone (PEEK) pellets (KetaSpire KT-820 NT SP) were bought from Solvay specialty polymers (Brussels, Belgium). These PEEK pellets have a diameter of approximately 2.5 mm. Sulfuric acid (S.G. 1.83, $\geq 95\%$) and p-xylene dichloride (98%) were purchased from Thermo Fisher Scientific (Geel, Belgium). Aluminum chloride (reagent grade, 98%) and N,N-dimethylacetamide (DMAc) were purchased from Sigma Aldrich (Hoeilaart, Belgium). All chemicals were used without further purification.

2.2. Membrane Synthesis

A schematic overview of the membrane preparation process is given in Figure 1. The PEEK polymer (3 g) was dissolved in 40 mL of concentrated sulfuric acid (95%) and stirred at 500 rpm on a hot plate stirrer at 60 °C/90 °C for 24 h. A 100 mL Duran® reagent bottle was used together with a 35 × 6 mm magnetic stirring rod. It is important to note that the degree of sulfonation depends on the dissolution rate of the pellets, which in turn depends on the stirring rate, sulfonation temperature and time, and dimensions of the recipient and stirring rod. sPEEK was obtained by precipitating the polymer solution in water. The sPEEK polymer was stirred in water for 24 h to remove impurities. Afterward, it was dried in a vacuum oven for 15 h at 60 °C. As preparation for the crosslinking step, a 100 mL three-necked flask was dried overnight at 60 °C and flushed with dry N₂ gas for 10 min. N,N-dimethylacetamide (DMAc) was added to the flask and flushed with dry N₂ gas for 10 min. No change in the volume of the solvent was observed. The total amount of solvent was equal to 7 mL per obtained gram of dry sPEEK-mass. AlCl₃ was added and stirred for five minutes, after which 1.68 g of the crosslinker dichloro-p-xylene (DCX) was added and stirred for ten minutes. The dry sPEEK polymer was added, and the solution was stirred for 6 h to obtain a homogeneous casting solution. The casting solution was cast on a glass plate at a thickness of 250 μm , and the solvent was evaporated in a vacuum oven at 60 °C for 2.5 h. The glass plate with the dry polymer film was put in an oven at elevated temperatures to perform the crosslinking reaction. The temperature and time for the crosslinking and sulfonation were different for each membrane type; Table 1 shows the synthesis details for every type. The synthesis of the non-crosslinked sulfonated membrane (sPEEK membrane) followed the abovementioned sulfonation step, after which the dry sPEEK polymer was dissolved in DMAc (7 mL DMAc/g sPEEK) and cast at 250 μm .

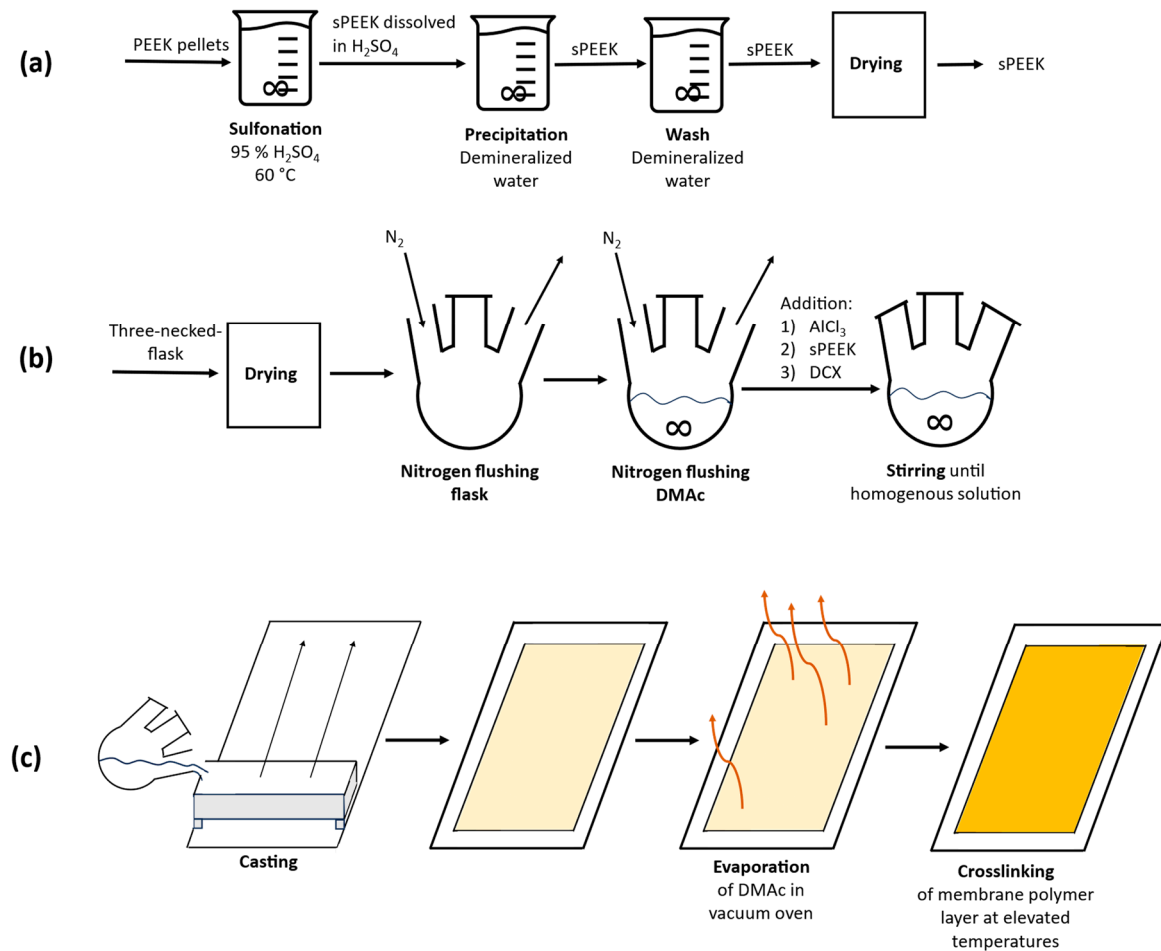


Figure 1. Schematic of the different steps for the membrane preparation. (a) Sulfonation of PEEK, (b) preparation of casting solution, (c) crosslinking of the membrane material.

Table 1. Specifications for the synthesis of the considered proton exchange membranes.

Membrane	Sulfonation Temperature (°C)	Sulfonation Time (h)	Crosslinking Temperature (°C)	Crosslinking Time (h)
sPEEK	60	24	/	/
sPEEK/DCX	60	24	140	15
sPEEK/DCX-s90°C	90	24	140	15
sPEEK/DCX-CX24h	60	24	140	24
sPEEK/DCX-CX190°C	60	24	190	15

2.3. Material Characterization

1. FTIR spectra of the membrane films were obtained with an FTIR Spectrometer (Spectrum 100, PerkinElmer, Waltham, MA, USA) in ATR mode using a diamond crystal (scan number = 4, resolution = 4 cm⁻¹).
2. The H-NMR spectrum was determined by dissolving 0.05 g sPEEK in 1 mL of deuterated DMSO. The H-NMR instrument (Bruker Avance III HD 400, Kontich, Belgium) was operated at 400 MHz. The degree of sulfonation was determined via the method of Arul Joseph Helen Therese et al. [31]:

$$\frac{n}{12 - 2n} = \frac{H_E}{H_A + H_B + H_C + H_D + H_{A'} + H_{B'}}$$

Degree of sulfonation (DS) = $n \cdot 100\%$ in which $H_A, H_B, H_{A'}, H_{B'}, H_C, H_D$ and H_E refer to the area below the peaks on the H-NMR spectrum corresponding to the aromatic hydrogens on position A, B, A', B', C, D and E, respectively. The identification of the aromatic hydrogen peaks is given in Figure 2 [31].

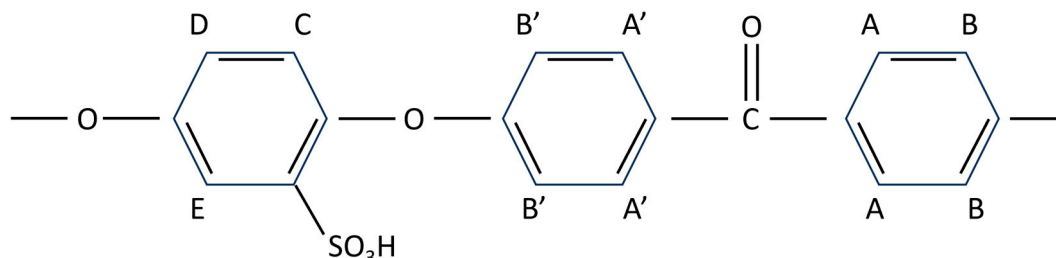


Figure 2. Identification of the different carbon types in a sPEEK backbone. The identification of the carbon types is used to calculate the degree of sulfonation [31].

- X-ray photoelectron spectroscopy (XPS) was carried out on a Kratos Axis SUPRAX-ray photoelectron spectrometer equipped with a charge neutralizer and a magnetic focusing lens, using Al K monochromated radiation (1486.7 eV). The surface charging of these samples was neutralized using a flood gun. All the spectra were fitted using CasaXPS, with energy referencing the C 1s peak. The background was corrected using a Shirley-type function.
- Scanning electron microscopy (SEM): To visualize the membrane structure and pore sizes, the membranes were analyzed using an SEM ULTRA (Zeiss). Membrane samples of approximately 1 cm^2 were placed on an SEM holder and sputter coated with a gold layer of 1.5 to 2 nm (BALZERS UNION FL 9460 BALZERS SCD 030). A voltage of 5 kV was used to obtain an image of the membrane surface. To evaluate the cross-section of the membrane, the membranes were repeatedly dipped in deionized water and consecutively immersed in liquid nitrogen. At these low temperatures, the membranes became brittle and could be broken without deforming the cross-section. A gold coating was also applied to these samples before the SEM analysis [32].

2.4. Membrane Parameters

- Ion exchange capacity: The dry mass of the membranes was measured on an analytical balance, and the sample was immersed in a 12 v% HCl solution for 48 h to protonate the sulfonic acid groups. The membrane samples and storage bottles were thoroughly washed with Milli-Q water before immersing the samples in a 1 M NaCl solution for 48 h. The protons in this NaCl solution were titrated with a 0.5 M NaOH solution using phenolphthalein as the indicator. The IEC was calculated using the following formula:

$$\text{IEC (mmol/g)} = \frac{c_{\text{NaOH}} \cdot V_{\text{NaOH}}}{m}$$

in which c_{NaOH} , V_{NaOH} and m are the concentration of NaOH (mmol/L), the volume of NaOH used during the titration (l) and the mass of the tested membrane sample (g), respectively.

- Water and methanol uptake: The membrane samples were dried for 20 h at $55 \text{ }^\circ\text{C}$, and the dry membrane mass was determined. Afterward, the membranes were soaked in pure water/methanol for 24 h. The membranes were taken out of the corresponding bath, excess liquid droplets were removed from the surface using a paper towel, and the mass of the membrane samples was determined. The uptake was calculated as follows:

$$\text{Water uptake (\%)} = \frac{m_{\text{water}}}{m_{\text{dry}}} \cdot 100 - 100$$

$$\text{Methanol uptake (\%)} = \frac{m_{\text{methanol}}}{m_{\text{dry}}} \cdot 100 - 100$$

in which m_{dry} is the weight of the dry membrane sample (g), and m_{water} and m_{methanol} are the membrane mass (g) after being soaked for 24 h in water and methanol, respectively.

3. The cation/anion permeation of the membranes was determined following the same procedure as reported by Deboli et al. and Firganek et al. [33,34]. First, the membrane was immersed in a 0.1 M KCl solution for 24 h. To perform the experiment, the membrane (active area 19.63 cm²) was positioned in a two-compartment cell equipped with two saturated calomel electrodes. The donor compartment was filled with a 0.5 M KCl solution and the receiving cell with a 0.1 M KCl solution. The potential difference over the membrane was measured by means of the potentiostat Origaflex 01A from Orignalys (France). The setup was left unattended until a stable value was reached (approximately 5 to 10 min). The cation/anion permeation was calculated, dividing the experimental potential difference (V_{exp}) by the theoretical potential difference (V_{theor}), as can be seen in the following equation:

$$\alpha (\%) = \frac{\Delta V_{\text{exp}}}{\Delta V_{\text{theor}}} \cdot 100$$

The same experiment was performed using a combination of 0.1 M NaHCO₃ and 0.5 M NaHCO₃. The theoretical potential difference was calculated with the Nernst equation using the appropriate activity coefficients and was equal to 36.47 mV and 36.13 mV for the experiment using KCl and NaHCO₃, respectively [35,36].

2.5. Performance Testing

1. Methanol diffusion coefficient and permeability: To measure the methanol crossover of the membrane, the membrane was first soaked in water for 24 h. Then, the membrane was placed in a two-compartment diffusion cell. Both compartments had the same dimensions, having a thickness of 1 cm and a circular cross-section with a diameter of 6 cm. The concentrate side was filled with a 2 M methanol solution and the dilute side with demineralized water. The setup was left unattended for 90 min to make the methanol diffuse through the membrane. The compartments were emptied in separate beakers and the solutions were intensely mixed before taking three samples of 20 μ L. It is important to note that the mixing of the solution is crucial since methanol-water mixtures can have microscopic configurational inhomogeneities [37]. The methanol concentration of the samples was analyzed via GC-FID (TurboMatrix HS 40, PerkinElmer), with helium as the carrier gas. The methanol diffusion coefficient [38] and the methanol permeability are calculated as follows:

$$\text{Methanol diffusion coefficient : } D \left(\text{cm}^2/\text{min} \right) = \frac{\Delta C}{t \cdot C_0} \frac{V_B \cdot L}{A}$$

$$\text{Methanol permeability } P \left(1/\text{min} \right) = \frac{\Delta C}{t \cdot C_0}$$

ΔC , t and C_0 are the average concentration changes in the concentrate and dilute compartment (mol/L), time of the experiment (min) and the methanol concentration of the concentrate compartment at the start (mol/L), respectively. V_B , L and A represent, respectively, the volume in the dilute compartment (cm³) (which is similar to the concentrate compartment), the thickness of the membrane (cm) and the surface area of the membrane (cm²). The diffusion coefficient D describes the diffusion of methanol through the membrane, normalized by membrane surface area and by membrane thickness. Therefore, this parameter gives insight into the performance of the membrane material since the thickness of the membrane does not influence this parameter. The permeability parameter P describes the methanol crossover through the complete membrane. The membrane thickness does have an influence

on this parameter; therefore, the methanol permeability represents a more general membrane performance.

- Proton resistance: AC impedance spectroscopy with a frequency range from 200 kHz to 1 Hz and an oscillating voltage between -10 and 10 mV (Biologic Sp-150 instrument) was used to determine the proton resistance of the membranes. Before performing the experiment, the membrane was soaked in a 1 M H_2SO_4 solution for 24 h. The membrane (active area = 1 cm²) was put in a two-compartment cell sandwiched between two platinum electrodes. During the experiment, a 1 M H_2SO_4 solution was pumped through both compartments at a flow rate of 49 mL/min. The blank measurement was performed following the same procedure without the membrane. The resistance value was derived from the intersect at high frequencies on a complex impedance plane with the $\text{Re}(Z)$ axis. The proton resistance normalized by thickness was obtained by dividing that resistance value by the membrane thickness.

3. Results

3.1. Membrane Synthesis

Since the sulfonation of the PEEK polymer only occurs when it is dissolved, the dissolution rate is crucial for reproducibility. Using the procedure as described in Section 2.2, the polymer was fully dissolved after approximately five hours. The sulfonation reaction is an electrophilic substitution reaction in which sulfonic acid groups attach to carbon atoms showing the highest electron density [39]. The targeted sulfonation reaction is shown in Figure 3. During the washing of the polymer, the sPEEK that was sulfonated at 90 °C for 24 h partially dissolved in water. This is due to the increased hydrophilicity of the polymer after the sulfonation reaction. Therefore, extra attention has to be given to the washing of the polymer in order to avoid losses, e.g., by lowering the temperature of the washing water or by performing an additional filtration step after the washing step. Furthermore, flushing of the flask and solvent (DMAc) with N_2 before adding the AlCl_3 is crucial because of the reactive behavior of AlCl_3 with water.

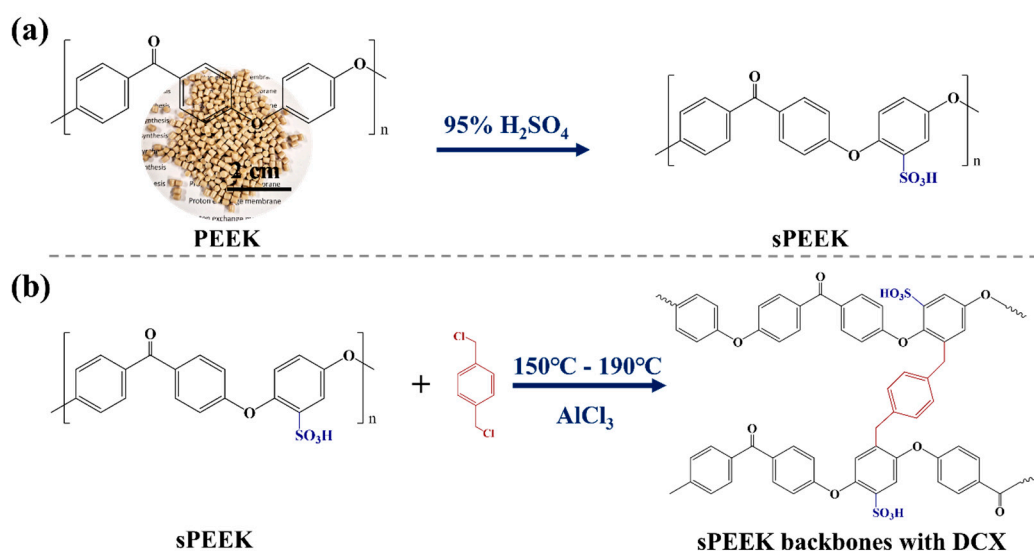


Figure 3. (a) The sulfonation reaction of PEEK into sPEEK, (b) the crosslinking reaction of the sPEEK with DCX via Friedel–Crafts.

The synthesis procedure resulted in thin, semi-transparent films with a thickness of around 20 μm in the dry state. The obtained membranes can be seen in the Supporting Information (Figure S1). All the membranes, except for the non-crosslinked sPEEK membrane, did not dissolve after immersion in DMAc for 72 h, indicating a crosslinked polymer structure. The crosslinking followed the Friedel–Crafts mechanism using AlCl_3 as the catalyst and p-xylylene dichloride (DCX) as the crosslinker. Figure 3 illustrates the targeted

sulfonation and crosslinking reaction. During this reaction, the carbon atoms with the highest electron density are again most favorable to bind with the crosslinker. Since the crosslinking reaction targets the same carbon atoms as the sulfonation, the crosslinking degree will be influenced by the sulfonation degree. A higher sulfonation degree lowers the availability of carbons on which the crosslinking can occur. Therefore, the crosslinking properties cannot be understood without taking the sulfonation into account.

3.2. Membrane Characterization

The H-NMR spectra of sPEEK sulfonated at 60 °C for 24 h is shown in Figure 4a. The same peaks, corresponding to the aromatic hydrogen peaks as in the work of Arul Joseph Helen Therese et al. [31], were observed, i.e., at 7.88–7.7 ppm (A, A'), 7.56–7.5 ppm (E) and 7.31–6.92 ppm (C, D, B, B'). The hydrogen E peak corresponds to the hydrogen of the -SO₃H group. After sulfonation at 60 °C for 24 h, a sulfonation degree of 65% was reached.

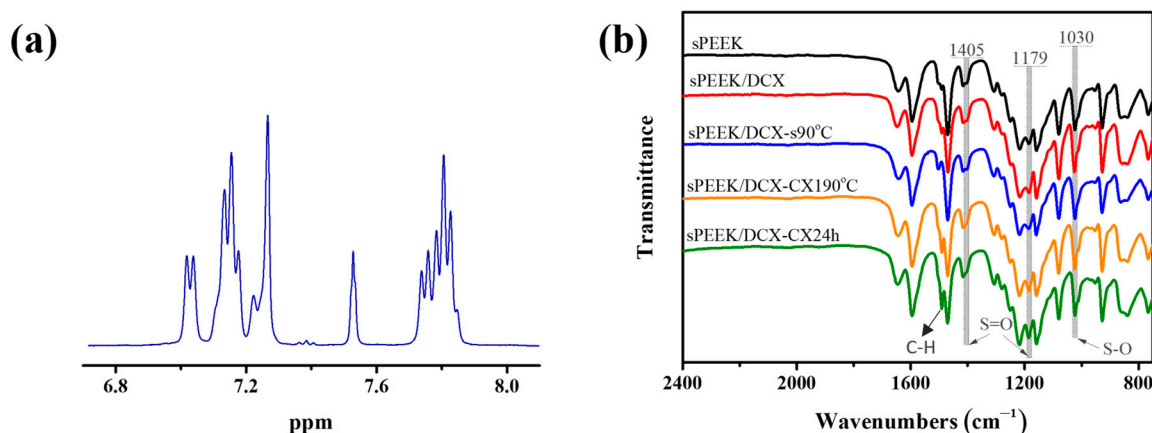


Figure 4. (a) NMR images of sPEEK; (b) FTIR images of the membranes synthesized in this work.

FTIR analysis was used to obtain a qualitative confirmation of the sulfonation of PEEK in the crosslinked membranes. Figure 4b shows the FTIR spectra of sPEEK and the four crosslinked sPEEK membranes. Peaks originating from the PEEK backbone are present in the fingerprint region of the spectra. The peak at 1648 cm⁻¹ belongs to the C=O group in the backbone, whilst the peaks at 1595 cm⁻¹ and 1415 cm⁻¹ correspond to skeletal ring vibrations. The peak at 1307 cm⁻¹ shows the bending motion of the C-C(=O)-C group, while the peak at 1185 cm⁻¹ is due to asymmetric stretching of the diphenyl ether group. The peaks at 1217 cm⁻¹ and 1159 cm⁻¹ show the aromatic hydrogens in plane deformation, and the peak at 928 cm⁻¹ refers to the aromatic hydrogens out of plane bending mode. The presence of the sulfonic acid groups is confirmed due to the presence of the peaks at 1080 and 1030 cm⁻¹, which correspond to the symmetric stretching of O=S=O and the stretching vibrations of S=O, respectively. The split peaks in the range between 860 and 840 cm⁻¹ are due to the isolated hydrogen in a 1,2,4-trisubstituted ring [40]. In addition, the peaks at 1179 and 1405 cm⁻¹ correspond to the S=O bond [41–43]. Furthermore, the intensity of the peak around 1480 cm⁻¹ is more enhanced for the membranes sPEEK/DCX-CX190°C and sPEEK/DCX-CX24h. Since this peak is located at the edge of the fingerprint region, it might correspond to the C-H bond of a methylene group. A methylene group would only be present in this membrane structure when the crosslinking reaction has occurred (see Figure 3). This would indicate that those two membrane types have an enhanced crosslinking. However, the quantitative determination of the crosslinking degree via the FTIR analysis remains complex, and the main focus of the FTIR analysis is the qualitative confirmation of the presence of sulfonic acid groups.

The surface and cross-section SEM images of the considered membranes in this work are shown in Figures 5 and 6, respectively. Based on both figures, it can be stated that the membrane surfaces are smooth without defects, holes, or pores. However, the membranes

became brittle due to the dry conditions during the SEM sample preparation and analysis. The brittleness made the membranes very sensitive to cracks during the handling. Those cracks can be seen in the cross-section image and show the importance of handling the membranes in wet conditions. Furthermore, the intensity of the peak around 1480 cm^{-1} is more enhanced for the membranes sPEEK/DCX-CX190°C and sPEEK/DCX-CX24h. Since this peak is located at the edge of the fingerprint region, it might correspond to the C-H bond of a methylene group. A methylene group would only be present in this membrane structure when the crosslinking reaction has occurred (see Figure 3). This would indicate that those two membrane types have an enhanced crosslinking. However, the quantitative determination of the crosslinking degree via the FTIR analysis remains complex, the main focus of the analysis is the qualitative confirmation of the presence of sulfonic acid groups.

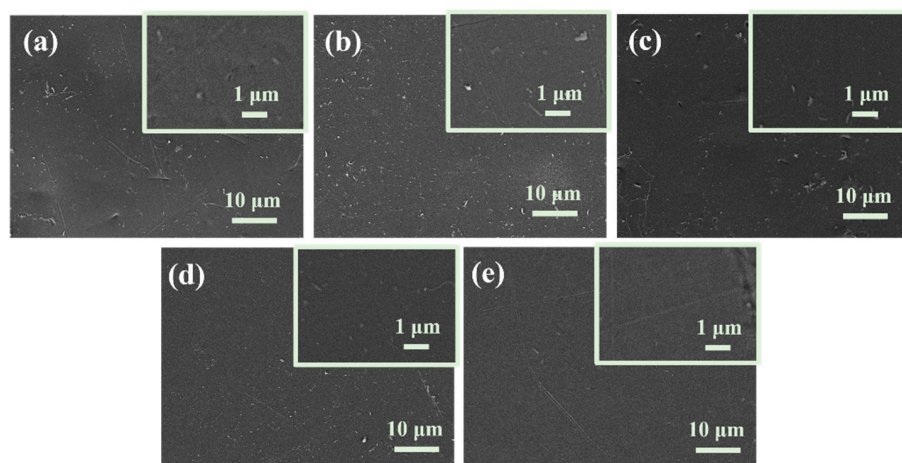


Figure 5. SEM images of the membrane surface of (a) sPEEK, (b) sPEEK/DCX, (c) sPEEK/DCX-s90°C, (d) sPEEK/DCX-CX24h, and (e) sPEEK/DCX-CX190°C.

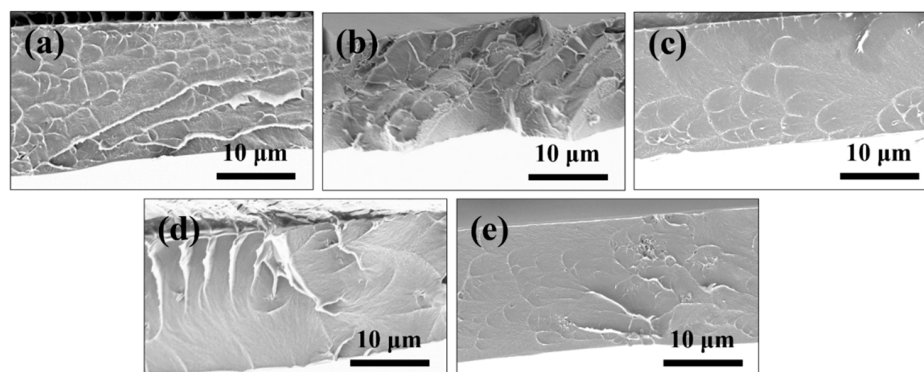


Figure 6. SEM images of the membrane cross-section of (a) sPEEK, (b) sPEEK/DCX, (c) sPEEK/DCX-s90°C, (d) sPEEK/DCX-CX24h, and (e) sPEEK/DCX-CX190°C.

Photoelectron spectroscopy (XPS) analysis was performed on the synthesized membranes to investigate the surface elemental composition before and after crosslinking with DCX. Figures 7 and 8 show the high-resolution XPS of C 1s and S 2p of the considered membranes, respectively. The spectra of O 1s can be found in the Supporting Information in Figure S2. The main constituents in the sPEEK sample were carbon and sulfur in the ionomer and oxygen in the ketone and ether linkages. The high-resolution C 1s spectra of the non-crosslinked sPEEK were fitted to four peaks with binding energies of about 284.6, 284.9, 286.3, and 288.2 eV (Figure 7a,b). The peak at 284.6 eV was assigned to the aryl C=C network, whereas the peaks at 284.9, 286.9, and 288.2 eV corresponded to alkyl (C-H), C-O-C/C-S, and carboxyl (C=O) groups, respectively [44–46]. A peak corresponding to C-C bonds appeared in the spectra of all membranes crosslinked with DCX (Figure 7c–f),

whereas the intensity of the C-O and C=O peaks decreased. As can be seen in Figure 3, DCX is the only source of sp³ carbons (C-C) in the membrane polymer. The appearing C-C peak in Figure 7c–f, therefore, is only possible if crosslinking has occurred. Probably, the most interesting result from the XPS is that the sp²/sp³ carbon ratio gives information on the crosslinking degree of the polymer. More specifically, the lower the ratio, the higher the crosslinking degree. The ratios are given in Table 2. The sp²/sp³ ratio is the lowest for sPEEK/DCX-CX24h and sPEEK/DCX-CX190°C, which shows that a higher crosslinking time or temperature significantly increases the crosslinking degree. The sp²/sp³ ratio of sPEEK/DCX-CXs90 is higher than sPEEK/DCX due to its lack of crosslinking sites, which is caused by the high degree of sulfonation. As these membranes were kept in water, a broad peak at 288.5–289.0 eV, corresponding to surface carbonates, was found mainly in the C 1s spectra of sPEEK/DCX-CX24h membranes, which could be attributed to physisorption of dissolved CO₂ [47].

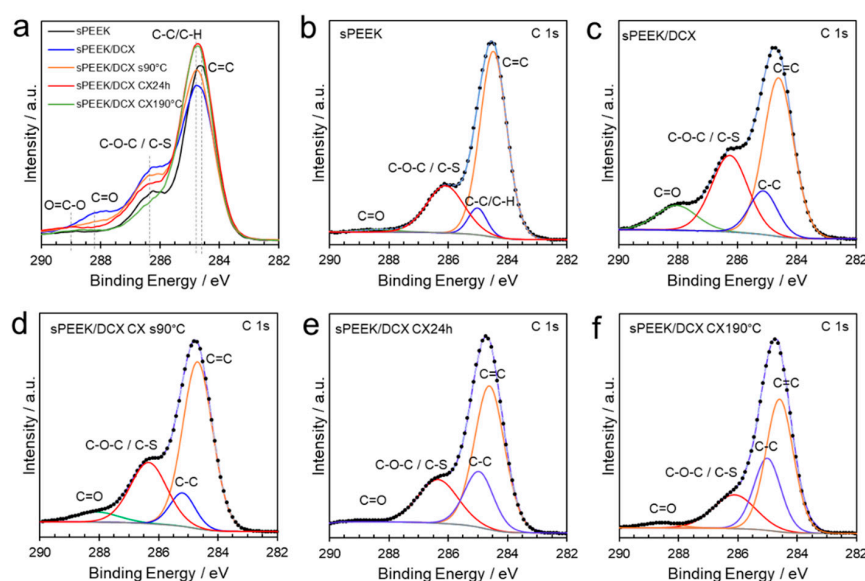


Figure 7. High-resolution C 1s XPS spectra of the synthesized membranes; (a) comparison of all membranes before deconvolution, (b) sPEEK, (c) sPEEK/DCX, (d) sPEEK/DCX-s90°C, (e) sPEEK/DCX-CX24, and (f) sPEEK/DCX-CX190°C.

Table 2. Quantification of C-C and C=C surface carbons.

Membrane	C 1s, Binding Energies (eV)		
	284.5 C=C	284.9 C-C	Ratio C=C/C-C
sPEEK	67.76	6.81	9.95
sPEEK/DCX	48.11	12.39	3.88
sPEEK/DCX-s90°C	58.60	9.88	5.93
sPEEK/DCX-CX24h	55.82	20.94	2.66
sPEEK/DCX-CX190°C	50.57	27.20	1.86

Figure 8 shows the S 2p spectra with two peaks at 168.2 and 169.5 eV, corresponding to 2p_{3/2} and 2p_{1/2} sulfur. No discernible difference could be found in the S 2p spectra between the non-crosslinked and crosslinked sPEEK membranes, demonstrating that crosslinking had no influence on the sulfonation of the polymer. As shown in Figure S2 in the Supporting Information, the O 1s signal was deconvoluted to the main peaks of C-O-C at 533.3 eV, C=O at 531.5 eV, and -SO₃H around 532 eV. The strong shoulder at a higher binding energy was seen primarily in the O 1s spectra of sPEEK/DCX-CX24h and

sPEEK/DCX-CX190°C membranes, which could be attributed to the physical adsorption of dissolved H₂O/CO₂. This is in agreement with the carbon O 1s spectra [47].

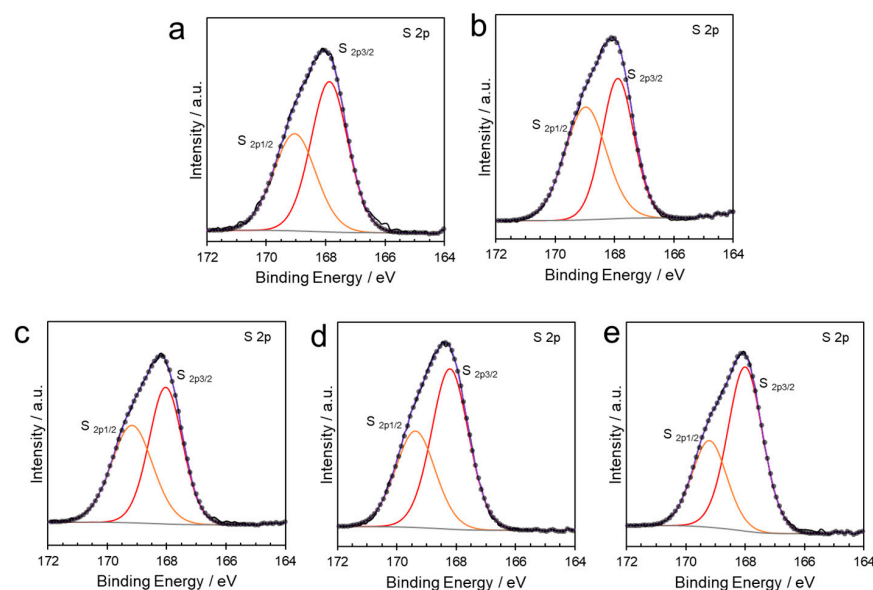


Figure 8. High-resolution S 2p XPS spectra of the synthesized membranes; (a) sPEEK, (b) sPEEK/DCX, (c) sPEEK/DCX-CXs90°C, (d) sPEEK/DCX-CX24h, and (e) sPEEK/DCX-CX190°C.

3.3. Membrane Parameters

The ion exchange capacity (IEC) shows the amount of sulfonic acid groups per gram of dry membrane mass. These groups are responsible for the transport of cations through the membrane. The higher the IEC, the higher the proton conductivity. Figure 9a shows the IEC of Nafion 117 compared to the membranes synthesized in this study. The IEC of Nafion 117 (1.04 mmol/g) agrees with the values found in reference [48]. The results show that all the crosslinked sPEEK membranes show a higher IEC, which indicates that the sulfonation with concentrated H₂SO₄ for 24 h at 60 °C led to a sufficient number of functional groups. Increasing the sulfonation temperature to 90 °C triples the IEC compared to Nafion 117. Furthermore, the IEC decreases with increasing crosslinking density since the crosslinker increases the membrane mass without adding sulfonic acid groups. Figure 9b,c show the water and methanol uptake of the synthesized membranes compared to Nafion 117, respectively. The non-crosslinked sPEEK membrane is very hydrophilic and not dense due to the absence of DCX and, therefore, has the highest uptake values. However, the uptake values decrease with increasing crosslinking degree. For example, sPEEK/DCX-s90°C has relatively high uptake values due to its high sulfonation degree and limited crosslinking degree. Increasing the crosslinking degree further by increasing the crosslinking time (sPEEK/DCX-CX24h) and temperature (sPEEK/DCX-CX190°C) eventually leads to uptake values even lower than the commercial benchmark. Those membranes are very dense, making them more resistant to swelling, and contain more hydrophobic regions, which reject water and methanol.

Cation/anion permeation: Figure 10 shows the cation/anion permeation of Nafion 117 and the membranes of this study, tested for KCl (a) and NaHCO₃ (b). The crosslinking degree has the largest influence on this performance parameter. The non-crosslinked sPEEK and the poorly crosslinked sPEEK/DCX-s90°C almost had no selectivity when KCl was used (16 and 33%, respectively) and a very poor selectivity when NaHCO₃ was used (47 and 56%, respectively), despite having a high IEC. These results indicate that the electrostatic repulsion forces coming from the sulfonic acid groups are not sufficient to inhibit the anions from permeating through the thin, non-dense membrane. Since the higher sulfonation temperature led to fewer available crosslinking sites, a sulfonation temperature of 60 °C was considered optimal for this study. Crosslinking the membranes

led to a higher cation/anion permeation due to the presence of more hydrophobic regions formed by DCX and a denser structure. This could also be linked to the lower water and methanol uptake values. The sPEEK/DCX membrane showed selectivity ratios of 66 and 74% when using KCl and NaHCO₃, respectively. Although these values are higher than sPEEK and sPEEK/DCX-s90°C, they are still inferior to Nafion 117, which has selectivity values of 91 and 84% for KCl and NaHCO₃, respectively. However, the selectivity values become comparable with the commercial benchmark when the crosslinking density is further increased. sPEEK/DCX-CX24h has selectivity ratios of 85 and 86% for KCl and NaHCO₃, respectively, and sPEEK/DCX-CX190°C has selectivity ratios of 87 and 81% for KCl and NaHCO₃, respectively. Therefore, a sufficiently crosslinked membrane can reach competitive selectivities compared to the commercial benchmark.

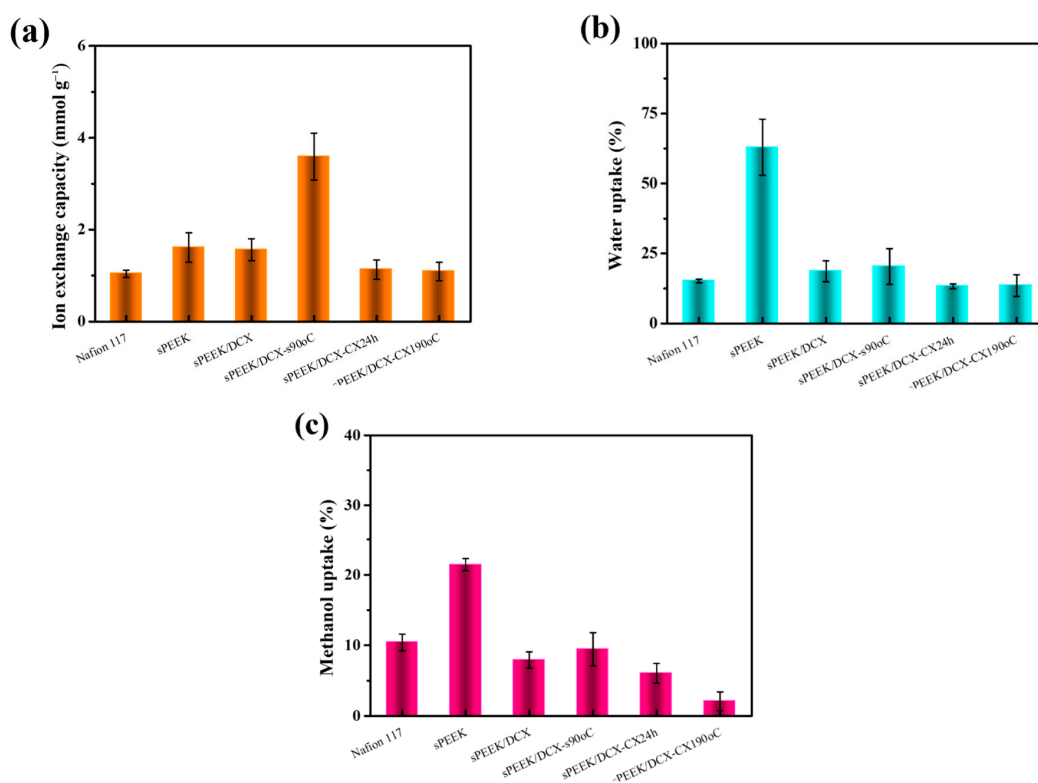


Figure 9. (a) Ion exchange capacity, (b) the water uptake, and (c) the methanol uptake.

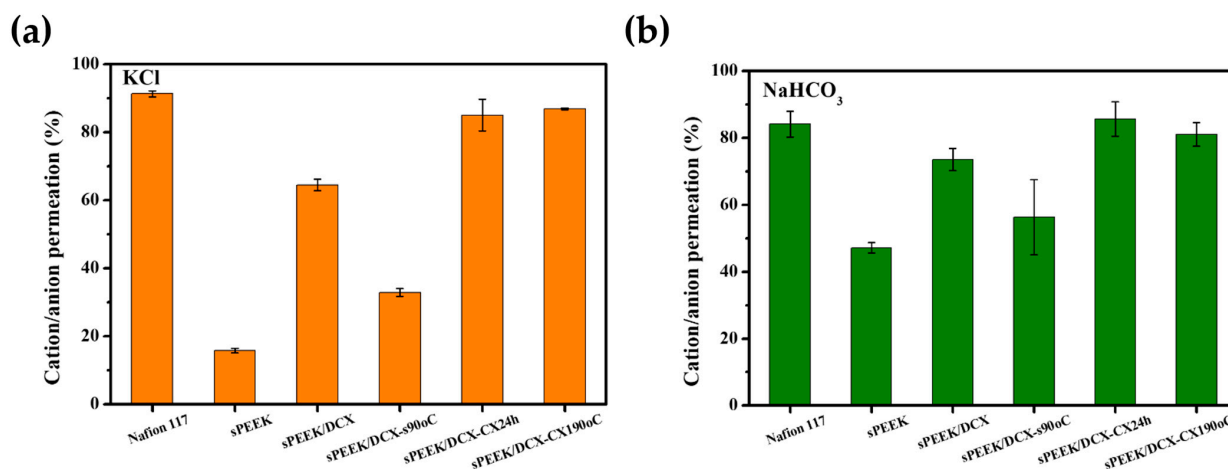


Figure 10. Cation/anion permeation of Nafion 117 compared to the synthesized membranes; (a) KCl cation/anion permeation, (b) NaHCO₃ cation/anion permeation.

3.4. Performance Testing: Proton Resistance/Methanol Diffusivity

As mentioned before, very often, a trade-off has to be made between methanol rejection and proton conductivity when considering PEMs for applications in DMFCs and artificial photosynthesis. Figures 11 and 12 show those two key performance parameters for Nafion 117 and the PEMs of this study. The methanol permeation data and the proton resistance values in Figure 11 are normalized by thickness and surface area. A thickness of 183 μm is assumed for Nafion 117, and the measured thickness of 20 μm is used for the PEMs of this study. Due to the normalization, Figure 11 shows the intrinsic properties of the membrane material without the influence of the membrane thickness. The most important observations are the lower resistance of the Nafion 117 membrane and the superior methanol diffusion coefficient of the PEMs of this study. These results are in line with the expectations. The morphology of Nafion consists of connected ionic clusters that serve as proton conducting channels [8], leading to high conductivity, while sPEEK-based membranes are known to have limited conductivities [49]. The relatively high standard deviations for the proton resistance come from the high sensitivity of the measurement values due to the low membrane resistance (see Figure 12) and low membrane thickness.

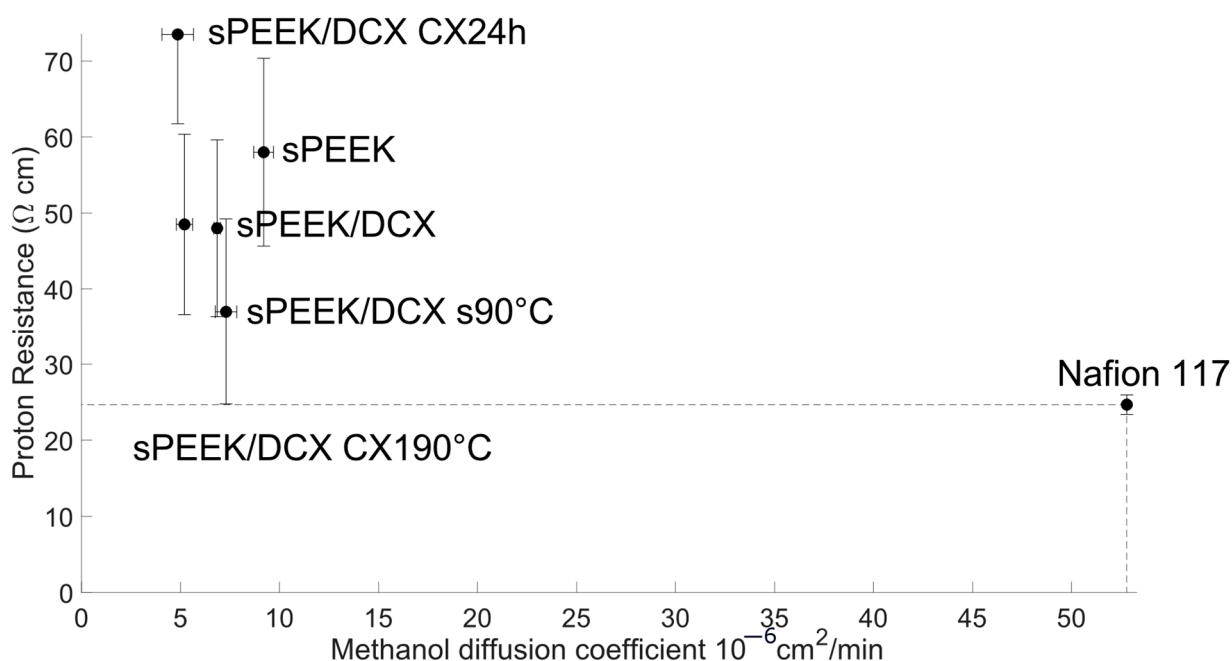


Figure 11. Proton resistance versus methanol diffusion coefficient of Nafion 117 and the synthesized membranes, all normalized by the thickness.

The shortcoming of the methodology of how the data are represented in Figure 11 is that it gives the impression that the membrane performance can easily be tuned by the thickness. However, a different membrane morphology will be formed during the solvent evaporation step if a thicker membrane is cast. Therefore, the membrane performance does not change linearly with the membrane thickness. A better way to compare the results of the synthesized PEMs of this study with Nafion 117 is via Figure 12. In Figure 12, the parameters are not normalized by the membrane thickness such that the effect of the low membrane thickness becomes visible. The methanol permeability and the proton resistance of Nafion 117 are indicated with a dotted line. Similar results in the literature were obtained for the proton resistance of Nafion 117 (see Napoli et al. [50]), indicating the validity of this approach. Their study showed an average proton conductivity of 0.0605 S/cm, tested in 1 M H_2SO_4 , compared to 0.0407 S/cm in this study. The difference between the two values can be explained by a different setup and different pretreatments. The conversion from the measured 0.45 $\Omega \text{ cm}^2$ in this study to 0.0407 S/cm follows the calculations explained

by Napoli et al. [50], including 183 μm as the thickness for Nafion 117. The results from the electrochemical impedance spectroscopy are shown in the Supporting Information in Figure S3. The membrane proton resistance equals the intersect at high frequencies on the complex impedance plane with the $\text{Re}(Z)$ axis. Figure 12 shows that although the proton resistance normalized by the membrane thickness of Nafion 117 is lower than the PEMs of this study, once the membrane thickness is taken into account, all sPEEK membranes have superior proton resistance values. The low thickness of the membranes in combination with the high IEC explains this significantly lower membrane resistance. In summary, the membranes with the lowest and highest resistance are, respectively, sPEEK/DCX-s90°C, which is sulfonated at the highest temperature, and sPEEK/DCX-CX24h, which has one of the highest crosslinking degrees. However, the difference in conductivities is limited.

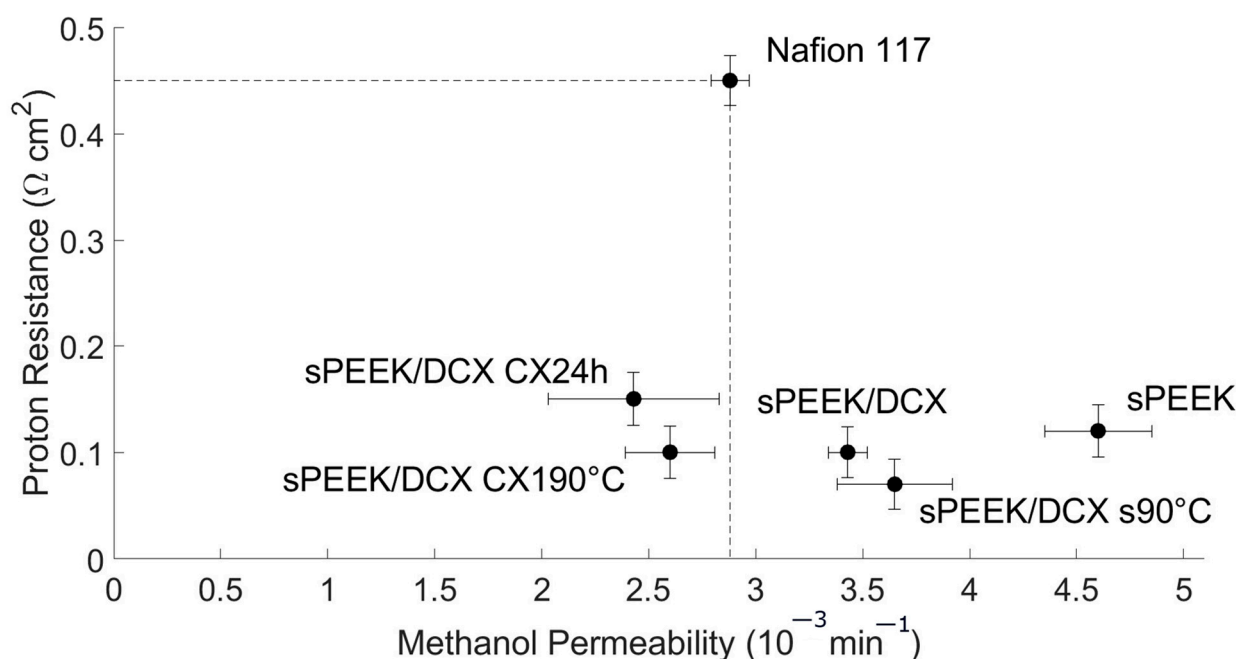


Figure 12. Proton resistance versus methanol permeation of Nafion 117 and the synthesized membranes.

The crosslinking degree has the largest influence on the methanol permeability. The non-crosslinked sPEEK membrane has a methanol permeability more than 50% higher than the commercial benchmark. Introducing some crosslinking (sPEEK/DCX and sPEEK/DCX-s90°C) lowers the methanol permeability, but competitive values are not reached. Additionally, sPEEK/DCX-s90°C has a slightly higher methanol permeability compared to sPEEK/DCX, as sPEEK/DCX-s90°C has a lower crosslinking degree due to a higher degree of sulfonation. However, sPEEK/DCX-CX24h and sPEEK/DCX-CX190°C are the two best-performing membranes. They both fall within the rectangular area, meaning that they have an improved proton resistance and methanol rejection compared to the commercial benchmark. The lower methanol permeability can be explained by the high crosslinking degree, which makes the membrane dense and less permeable for methanol. In addition, the presence of DCX creates hydrophobic parts, rejecting methanol. Those effects were also consistent with the lower water and methanol uptake values [34].

4. Conclusions

Crosslinked sPEEK PEMs were fabricated using a facile fabrication process with low-cost and non-hazardous chemicals, with the aim of overcoming the traditional trade-off between methanol rejection and proton conductivity. The highly sulfonated PEEK backbones were crosslinked via a Friedel–Crafts reaction with the hydrophobic monomer p-xylylene dichloride (DCX). The crosslinked PEMs did not dissolve in DMAc, confirming a successful crosslinking. The membranes were optimized by varying the sulfonation

and crosslinking intensities. A sulfonation temperature of 60 °C resulted in a sulfonation degree of 56% and IECs higher than Nafion 117. A higher sulfonation temperature of 90 °C (sPEEK/DCX-s90°C) even led to an IEC of more than 3.5 mmol/g; however, at that degree of sulfonation, sPEEK became soluble in water, which is a practical issue. Furthermore, the sPEEK/DCX-s90°C had fewer available crosslinking spots due to the higher sulfonation degree, resulting in a lower performance. Therefore, a sulfonation temperature of 60 °C was considered to be optimal. In addition, all the PEMs showed lower proton resistance values than the commercial benchmark, which can be explained by the low thickness and the high IECs. The amount of crosslinking was controlled by varying the crosslinking time and temperature, and the crosslinking degree was measured using XPS. The crosslinking degree had a significant effect on the water and methanol uptake, cation/anion permeation, and methanol permeability. An increase in crosslinking degree makes the membrane more dense and, hence, less permeable for all solutes. Furthermore, since DCX is hydrophobic, it increases the hydrophobic character of the membrane, which rejects specific compounds, such as water and methanol. Due to those effects, the highly crosslinked membranes, i.e., sPEEK/DCX-CX24h and sPEEK/DCX-CX190°C, showed high performances, i.e., low water- and methanol uptake values, high cation/anion permeation and a low methanol permeability, as opposed to the poorly crosslinked PEMs, i.e., sPEEK and sPEEK/DCX-s90°C.

In conclusion, it could be stated that both sPEEK/DCX-CX24h and sPEEK/DCX-CX190°C overcame the traditional trade-off between proton conductivity and methanol rejection. Both membrane types showed lower resistance and lower methanol permeability. Therefore, this work showed the possibility of using a facile fabrication procedure using non-hazardous compounds for the synthesis of PEMs, which are able to overcome the trade-off between proton conductivity and methanol rejection.

Supplementary Materials: The following supporting information can be downloaded at: <https://www.mdpi.com/article/10.3390/app14073089/s1>, Figure S1: Pictures of the sPEEK/DCX membranes; Figure S2: High-resolution O 1s XPS spectra of the self-synthesized membranes; (a) sPEEK, (b) sPEEK/DCX, (c) sPEEK/DCX-s90°C, (d) sPEEK/DCX-CX24h, (e) sPEEK/DCX-CX190°C; Figure S3: The impedance spectroscopy data of the proton resistance experiment. The resistance value is derived from the intersect at high frequencies on the complex impedance plane with the Re(Z) axis.

Author Contributions: Conceptualization, S.D. and B.V.d.B.; methodology, S.D., L.T., G.V.E., S.K. and B.V.d.B.; software, G.V.E., S.K. and G.H.; validation, S.D. and L.T.; investigation, S.D., L.T., G.V.E., S.K. and G.H.; resources, B.V.d.B. and G.H.; data curation, S.D., L.T. and S.K.; writing—original draft preparation, S.D., G.V.E. and B.V.d.B.; writing—review and editing, S.D. and B.V.d.B.; supervision, B.V.d.B. and G.H.; project administration, B.V.d.B. and G.H.; funding acquisition, B.V.d.B. and G.H. All authors have read and agreed to the published version of the manuscript.

Funding: This work is part of the HySolChem project, which has received funding from the European Union's Horizon 2020 research and innovation programme under grant agreement No 101017928. Georg Held and Santosh Kumar thank "the EPSRC National Facility for XPS (HarwellXPS)", operated by Cardiff University and UCL, under contract no. PR16195.

Data Availability Statement: The original contributions presented in the study are included in the article, further inquiries can be directed to the corresponding author.

Acknowledgments: The authors would like to thank Francesco Deboli and Daniel Firganek for their help in measuring the cation/anion permeation. Additionally, the authors would like to thank Ariana Bampouli and Quinten Goris for performing the NMR analyses and Venkataramana Rishikesan for their help in measuring the proton conductivity. Finally, the authors would like to thank Elena Brozzi for helping with the graphics and for joining the discussions about the work.

Conflicts of Interest: Authors Santosh Kumar and Georg Held were employed by the company Diamond Light Source Ltd. The remaining authors declare that the research was conducted in the absence of any commercial or financial relationships that could be construed as a potential conflict of interest.

References

1. Omer, A.M. Energy, environment and sustainable development. *Renew. Sustain. Energy Rev.* **2008**, *12*, 2265–2300. [[CrossRef](#)]
2. Kim, Y.S.; Pivovar, B.S. Polymer Electrolyte Membranes for Direct Methanol Fuel Cells. *Adv. Fuel Cells* **2007**, *1*, 187–234. [[CrossRef](#)]
3. Neburchilov, V.; Martin, J.; Wang, H.; Zhang, J. A review of polymer electrolyte membranes for direct methanol fuel cells. *J. Power Sources* **2007**, *169*, 221–238. [[CrossRef](#)]
4. Parekh, A. Recent developments of proton exchange membranes for PEMFC: A review. *Front. Energy Res.* **2022**, *10*, 956132. [[CrossRef](#)]
5. Okonkwo, P.C.; Belgacem, I.B.; Emori, W.; Uzoma, P.C. Nafion degradation mechanisms in proton exchange membrane fuel cell (PEMFC) system: A review. *Int. J. Hydrogen Energy* **2021**, *46*, 27956–27973. [[CrossRef](#)]
6. Chabi, S.; Papadantonakis, K.M.; Lewis, N.S.; Freund, M.S. Membranes for artificial photosynthesis. *Energy Environ. Sci.* **2017**, *10*, 1320–1338. [[CrossRef](#)]
7. Mauritz, K.A.; Moore, R.B. State of Understanding of Nafion. *Chem. Rev.* **2004**, *104*, 4535–4586. [[CrossRef](#)] [[PubMed](#)]
8. Karimi, M.B.; Mohammadi, F.; Hooshyari, K. Recent approaches to improve Nafion performance for fuel cell applications: A review. *Int. J. Hydrogen Energy* **2019**, *44*, 28919–28938. [[CrossRef](#)]
9. Hickner, M.A.; Ghassemi, H.; Kim, Y.S.; Einsla, B.R.; McGrath, J.E. Alternative Polymer Systems for Proton Exchange Membranes (PEMs). *Chem. Rev.* **2004**, *104*, 4587–4612. [[CrossRef](#)]
10. Wang, R.; Zhang, W.; He, G.; Gao, P. Controlling fuel crossover and hydration in ultra-thin proton exchange membrane-based fuel cells using Pt-nanosheet catalysts. *J. Mater. Chem. A* **2014**, *2*, 16416–16423. [[CrossRef](#)]
11. Dicks, A.L. PEM Fuel Cells. In *Comprehensive Renewable Energy*; Elsevier: Amsterdam, The Netherlands, 2012; pp. 203–245. [[CrossRef](#)]
12. Grot, W. Manufacture. In *Fluorinated Ionomers*; Elsevier: Amsterdam, The Netherlands, 2011; pp. 11–48. [[CrossRef](#)]
13. Feng, M.; Qu, R.; Wei, Z.; Wang, L.; Sun, P.; Wang, Z. Characterization of the thermolysis products of Nafion membrane: A potential source of perfluorinated compounds in the environment. *Sci. Rep.* **2015**, *5*, 9859. [[CrossRef](#)] [[PubMed](#)]
14. Chen, H.; Yao, Y.; Zhao, Z.; Wang, Y.; Wang, Q.; Ren, C.; Wang, B.; Sun, H.; Alder, A.C. Multimedia Distribution and Transfer of Per- and Polyfluoroalkyl Substances (PFASs) Surrounding Two Fluorochemical Manufacturing Facilities in Fuxin, China. *Environ. Sci. Technol.* **2018**, *52*, 8263–8271. [[CrossRef](#)] [[PubMed](#)]
15. Zhou, J.; Baumann, K.; Surratt, J.D.; Turpin, B.J. Legacy and emerging airborne per- and polyfluoroalkyl substances (PFAS) collected on PM_{2.5} filters in close proximity to a fluoropolymer manufacturing facility. *Environ. Sci. Process Impacts* **2022**, *24*, 2272–2283. [[CrossRef](#)] [[PubMed](#)]
16. Depuydt, S.; Van der Bruggen, B. Green Synthesis of Cation Exchange Membranes: A Review. *Membranes* **2024**, *14*, 23. [[CrossRef](#)] [[PubMed](#)]
17. Zaidi, S.M.J.; Mikhailenko, S.D.; Robertson, G.P.; Guiver, M.D.; Kaliaguine, S. Proton conducting composite membranes from polyether ether ketone and heteropolyacids for fuel cell applications. *J. Memb. Sci.* **2000**, *173*, 17–34. [[CrossRef](#)]
18. Zhao, C.; He, D.; Li, Y.; Xiang, J.; Li, P.; Sue, H.-J. High-performance proton exchange membranes for direct methanol fuel cells based on a SPEEK/polybenzoxazine crosslinked structure. *RSC Adv.* **2015**, *5*, 47284–47293. [[CrossRef](#)]
19. Zhao, C.; He, D.; Yang, Q.; Li, Y.; Yue, J. Preparation and properties of semi-IPN proton exchange membranes based on SPEEK and cross-linked PSt-DVB for direct methanol fuel cells. *High. Perform. Polym.* **2017**, *29*, 1110–1117. [[CrossRef](#)]
20. Ramly, N.N.B.; Ali, A.M.M.B. The preparation and characterization of sulfonated poly (ether ether ketone) and Cellulose Acetate (SPEEK-CA) membrane in proton exchange membrane fuel cells (PEMFCs) by UV-crosslink technique. In Proceedings of the 2012 IEEE Colloquium on Humanities, Science and Engineering (CHUSER), Kota Kinabalu, Malaysia, 3–4 December 2012; pp. 637–641. [[CrossRef](#)]
21. Li, W.; Jiang, J.; An, H.; Dong, S.; Yue, Z.; Qian, H.; Yang, H. Self-Cross-Linked Sulfonated Poly(ether ether ketone) with Pendant Sulfoalkoxy Groups for Proton Exchange Membrane Fuel Cells. *ACS Appl. Energy Mater.* **2021**, *4*, 2732–2740. [[CrossRef](#)]
22. Zhong, S.; Cui, X.; Cai, H.; Fu, T.; Zhao, C.; Na, H. Crosslinked sulfonated poly(ether ether ketone) proton exchange membranes for direct methanol fuel cell applications. *J. Power Sources* **2007**, *164*, 65–72. [[CrossRef](#)]
23. Wang, R.; Liu, S.; Wang, L.; Li, M.; Gao, C. Understanding of Nanophase Separation and Hydrophilic Morphology in Nafion and SPEEK Membranes: A Combined Experimental and Theoretical Studies. *Nanomaterials* **2019**, *9*, 869. [[CrossRef](#)]
24. Xiao, T.; Wang, R.; Chang, Z.; Fang, Z.; Zhu, Z.; Xu, C. Electrolyte membranes for intermediate temperature proton exchange membrane fuel cell. *Progress. Nat. Sci. Mater. Int.* **2020**, *30*, 743–750. [[CrossRef](#)]
25. Lan, Y.; Huang, Y.; Zhou, D.; Zhang, X.; Xia, L.; Dewil, R.; Van der Bruggen, B.; Zhao, Y. Internally Cross-Linked Polysulfone-Based Anion Exchange Membranes with pH Stability for Carboxylate Separation. *ACS EST Water* **2023**, *3*, 4183–4194. [[CrossRef](#)]
26. Mirfarsi, S.H.; Parnian, M.J.; Rowshanzamir, S.; Kjeang, E. Current status of cross-linking and blending approaches for durability improvement of hydrocarbon-based fuel cell membranes. *Int. J. Hydrogen Energy* **2022**, *47*, 13460–13489. [[CrossRef](#)]
27. Deboli, F.; Van der Bruggen, B.; Donten, M.L. A novel concept of hierarchical cation exchange membrane fabricated from commodity precursors through an easily scalable process. *J. Membr. Sci.* **2021**, *636*, 119594. [[CrossRef](#)]
28. Samimi, F.; Rahimpour, M.R. Direct Methanol Fuel Cell. In *Methanol*; Elsevier: Amsterdam, The Netherlands, 2018; pp. 381–397. [[CrossRef](#)]
29. Loh, X.X.; Sairam, M.; Bismarck, A.; Steinke, J.H.G.; Livingston, A.G.; Li, K. Crosslinked integrally skinned asymmetric polyaniline membranes for use in organic solvents. *J. Membr. Sci.* **2009**, *326*, 635–642. [[CrossRef](#)]

30. Wang, K.Y.; Xiao, Y.; Chung, T.-S. Chemically modified polybenzimidazole nanofiltration membrane for the separation of electrolytes and cephalexin. *Chem. Eng. Sci.* **2006**, *61*, 5807–5817. [[CrossRef](#)]
31. Therese, J.A.J.H.; Selvakumar, K.; Gayathri, R.; Prabhu, M.R.; Sivakumar, P. In situ polymerization of poly aniline—SPEEK-PMA-based proton exchange membrane for DMFC application. *J. Thermoplast. Compos. Mater.* **2021**, *34*, 221–237. [[CrossRef](#)]
32. Li, W.; Molina-Fernández, C.; Estager, J.; Monbaliu, J.-C.M.; Debecker, D.P.; Luis, P. Supported ionic liquid membranes for the separation of methanol/dimethyl carbonate mixtures by pervaporation. *J. Membr. Sci.* **2020**, *598*, 117790. [[CrossRef](#)]
33. Deboli, F.; Van der Bruggen, B.; Donten, M.L. A versatile chemistry platform for the fabrication of cost-effective hierarchical cation and anion exchange membranes. *Desalination* **2022**, *535*, 115794. [[CrossRef](#)]
34. Firganek, D.; Donten, M.L.; Van der Bruggen, B. Impact of Formulation of Photocurable Precursor Mixtures on the Performance and Dimensional Stability of Hierarchical Cation Exchange Membranes. *Ind. Eng. Chem. Res.* **2023**, *62*, 15928–15939. [[CrossRef](#)]
35. Pitzer, K.S.; Peiper, J.C. Activity coefficient of aqueous sodium bicarbonate. *J. Phys. Chem.* **1980**, *84*, 2396–2398. [[CrossRef](#)]
36. Dash, D.; Kumar, S.; Mallika, C.; Mudali, U.K. New Data on Activity Coefficients of Potassium, Nitrate, and Chloride Ions in Aqueous Solutions of KNO₃ and KCl by Ion Selective Electrodes. *ISRN Chem. Eng.* **2012**, *2012*, 730154. [[CrossRef](#)]
37. Bakó, I.; Megyes, T.; Bálint, S.; Grósz, T.; Chihai, V. Water–methanol mixtures: Topology of hydrogen bonded network. *Phys. Chem. Chem. Phys.* **2008**, *10*, 5004. [[CrossRef](#)] [[PubMed](#)]
38. Zhong, S.; Cui, X.; Cai, H.; Fu, T.; Shao, K.; Na, H. Crosslinked SPEEK/AMPS blend membranes with high proton conductivity and low methanol diffusion coefficient for DMFC applications. *J. Power Sources* **2007**, *168*, 154–161. [[CrossRef](#)]
39. Huang, R.Y.M.; Shao, P.; Burns, C.M.; Feng, X. Sulfonation of poly(ether ether ketone)(PEEK): Kinetic study and characterization. *J. Appl. Polym. Sci.* **2001**, *82*, 2651–2660. [[CrossRef](#)]
40. Al Lafi, A.G. The sulfonation of poly(ether ether ketone) as investigated by two-dimensional FTIR correlation spectroscopy. *J. Appl. Polym. Sci.* **2015**, *132*. [[CrossRef](#)]
41. Zhao, Y.; Wu, M.; Shen, P.; Uytterhoeven, C.; Mamrol, N.; Shen, J.; Gao, C.; Van der Bruggen, B. Composite anti-scaling membrane made of interpenetrating networks of nanofibers for selective separation of lithium. *J. Membr. Sci.* **2021**, *618*, 118668. [[CrossRef](#)]
42. Zhao, Y.; Li, Y.; Zhu, J.; Lejarazu-Larrañaga, A.; Yuan, S.; Ortega, E.; Shen, J.; Gao, C.; Van der Bruggen, B. Thin and robust organic solvent cation exchange membranes for ion separation. *J. Mater. Chem. A Mater.* **2019**, *7*, 13903–13909. [[CrossRef](#)]
43. Zhao, Y.; Qiu, Y.; Mai, Z.; Ortega, E.; Shen, J.; Gao, C.; Van der Bruggen, B. Symmetrically recombined nanofibers in a high-selectivity membrane for cation separation in high temperature and organic solvent. *J. Mater. Chem. A Mater.* **2019**, *7*, 20006–20012. [[CrossRef](#)]
44. Zhu, Y.; Cao, Z.; Peng, Y.; Hu, L.; Guney, T.; Tang, B. Facile Surface Modification Method for Synergistically Enhancing the Biocompatibility and Bioactivity of Poly(ether ether ketone) That Induced Osteodifferentiation. *ACS Appl. Mater. Interfaces* **2019**, *11*, 27503–27511. [[CrossRef](#)]
45. Chu, P.K.; Li, L. Characterization of amorphous and nanocrystalline carbon films. *Mater. Chem. Phys.* **2006**, *96*, 253–277. [[CrossRef](#)]
46. Afroj, S.; Karim, N.; Wang, Z.; Tan, S.; He, P.; Holwill, M.; Ghazaryan, D.; Fernando, A.; Novoselov, K.S. Engineering Graphene Flakes for Wearable Textile Sensors via Highly Scalable and Ultrafast Yarn Dyeing Technique. *ACS Nano* **2019**, *13*, 3847–3857. [[CrossRef](#)] [[PubMed](#)]
47. Collado, L.; Reynal, A.; Fresno, F.; Barawi, M.; Escudero, C.; Perez-Dieste, V.; Coronado, J.M.; Serrano, D.P.; Durrant, J.R.; de la Peña O’Shea, V.A. Unravelling the effect of charge dynamics at the plasmonic metal/semiconductor interface for CO₂ photoreduction. *Nat. Commun.* **2018**, *9*, 4986. [[CrossRef](#)] [[PubMed](#)]
48. Xi, J.; Wu, Z.; Qiu, X.; Chen, L. Nafion/SiO₂ hybrid membrane for vanadium redox flow battery. *J. Power Sources* **2007**, *166*, 531–536. [[CrossRef](#)]
49. Meng, X.; Song, K.; Lv, Y.; Cong, C.; Ye, H.; Dong, Y.; Zhou, Q. SPEEK proton exchange membrane with enhanced proton conductivity stability from phosphotungstic acid-encapsulated silica nanorods. *Mater. Chem. Phys.* **2021**, *272*, 125045. [[CrossRef](#)]
50. Napoli, L.; Franco, J.; Fasoli, H.; Sanguinetti, A. Conductivity of Nafion[®] 117 membrane used in polymer electrolyte fuel cells. *Int. J. Hydrogen Energy* **2014**, *39*, 8656–8660. [[CrossRef](#)]

Disclaimer/Publisher’s Note: The statements, opinions and data contained in all publications are solely those of the individual author(s) and contributor(s) and not of MDPI and/or the editor(s). MDPI and/or the editor(s) disclaim responsibility for any injury to people or property resulting from any ideas, methods, instructions or products referred to in the content.